

Lithium Deposition Mechanism under Different Thermal Conditions Unraveled via an Optimized Phase Field Model

Guowei Tang, Libo Men, Yilin Wang, Rong Xu, and Yucan Peng*



Cite This: *Nano Lett.* 2025, 25, 2561–2567



Read Online

ACCESS |



Metrics & More



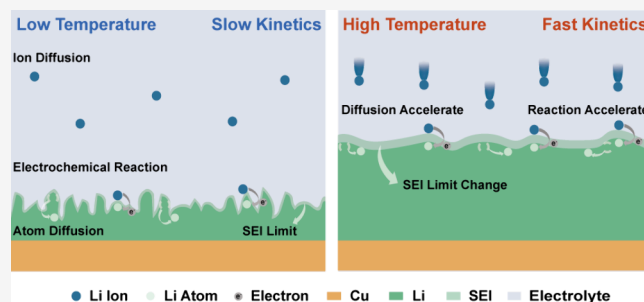
Article Recommendations



Supporting Information

ABSTRACT: As one of the most important physical fields for battery operation, the regulatory effect of temperature on the growth of lithium dendrites should be studied. In this paper, we develop an optimized phase field model to explore the effect of temperature on the growth of Li dendrites in Li metal batteries. We incorporated full lithium deposition kinetics, including atom diffusion and solid electrolyte interface restriction on interface kinetics, into the model and revealed their significance in determining the transformation of the lithium deposition morphology from moss-like to dendrite-like. We found that a high temperature or dispersed hot spots are more conducive to stable battery operation than a low temperature or concentrated hot spots due to the enhanced diffusion kinetics at the high temperature and the more uniform temperature distribution of dispersed hot spots. We believe our work can provide a useful tool for further exploring the thermal effect on stable lithium metal battery operation.

KEYWORDS: lithium deposition, solid electrolyte interface, phase field simulation, thermal regulation



Traditional lithium-ion batteries with graphite as the anode material are gradually approaching their theoretical energy density limit.^{1–3} As the demand for battery capacity in electric vehicles and various portable electronic devices is increasing, it is imperative to design high-energy density rechargeable batteries with high-theoretical capacity lithium metal as the electrode material.^{4–7} However, due to the high activity of lithium metal anodes, many performance and safety issues arise during the battery charging and discharging process.^{8–12} In particular, lithium dendrites formed during battery cycling not only will lead to the loss of active materials in the battery but may also pierce the separator and cause the battery to short circuit.^{8,13–15} These issues limit the performance, safety, and cycle life of lithium metal batteries.^{3,16–18} Therefore, solving the problem of lithium dendrite growth inside the lithium battery is one of the most critical and important issues. Much research has been carried out on the solid and interface problems related to dendrite growth.^{19–27}

As one of the most important physical fields for battery operation, the temperature field has a significant impact on dendrite nucleation, growth, and the solid electrolyte interface (SEI).^{28–36} For dendrite growth, Li et al. found that under a high current density, due to the self-heating inside the battery, the increase in the diffusion rate can promote the healing of lithium dendrites,²⁹ while Zhu et al. found that local hot spots inside the battery will cause local deposition acceleration, leading to the short circuit problem.⁸ In general, the temperature field mainly regulates the growth of dendrites by affecting the diffusion kinetics, reaction kinetics, and SEI

properties inside the battery.^{29,30,37–39} However, it is difficult to directly reveal the underlying mechanism through experiments.

The phase field method, as a mesoscale simulation tool, can be directly used to simulate the lithium deposition and further explore the underlying mechanism.^{38,40–42} Some previous works have explored the influence of temperature on dendrite growth considering the effect of temperature on the ion diffusion rate and electrochemical reaction rate.^{38,43} Recently, Zhang et al. used the phase field model to explore the effect of atom diffusion on the growth of a single dendrite, illustrating the important role of atom diffusion on the lithium deposition process.⁴¹ However, a comprehensive model that considers both full deposition kinetics and SEI restriction on interface kinetics for exploring the mechanism and evolution of lithium deposition is lacking.

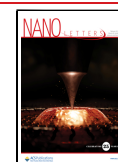
Herein, we optimized the previous phase field model to explore the influence of ion diffusion, electrochemical reaction, atom diffusion, and SEI restriction on lithium deposition morphology under different thermal conditions. We demonstrated the rationality and importance of introducing atom

Received: December 19, 2024

Revised: January 22, 2025

Accepted: January 24, 2025

Published: January 31, 2025



diffusion kinetics and SEI restriction on the direction of interface kinetics through simulating a single dendrite growth process. We have also deeply analyzed the process and mechanism of lithium deposition morphology transformation from moss-like to dendrite-like. In addition, the optimized phase field model was used to simulate the deposition results under different ambient temperatures and hot spot shapes and proved to be useful in exploring the lithium deposition mechanism under various conditions. We believe that our work

can provide a powerful tool for exploring lithium deposition mechanisms and the stable operation of lithium metal batteries.

The model in this paper is based on the nonlinear phase field model proposed by Yan et al. and the conservative Cahn–Hilliard equation.^{41,44–46} The detailed model is given in the [Supporting Information](#). The phase field equation is optimized in this paper to introduce the SEI restriction on the direction of interface kinetics and atom diffusion kinetics:

$$\begin{aligned} \frac{\partial \xi}{\partial t} = & \text{gradient energy} + \text{interfacial energy} + \text{atom diffusion energy} = L_{\sigma} \left\{ \nabla [\kappa(\theta) \nabla \xi] + \frac{1}{2} \frac{\partial}{\partial y} \left[\kappa'(\theta) \frac{\partial \xi}{\partial x} \right] - \frac{1}{2} \frac{\partial}{\partial x} \left[\kappa'(\theta) \frac{\partial \xi}{\partial y} \right] \right\} \\ & - \left(L_{\sigma} g'(\xi) + L_{\eta} h'(\xi) \left\{ \exp \left[\frac{(1-\alpha)nF\eta_{\alpha}}{RT} \right] - \tilde{c}_{+} \exp \left(\frac{-\alpha nF\eta_{\alpha}}{RT} \right) \right\} \right) (1 + \chi \psi) \\ & + \nabla \left\{ \frac{D_{\text{Li},T} V_m \xi}{RT} \nabla [2W\xi(2\xi - 1)(\xi - 1) - \nabla(k_0 \nabla \xi)] \right\} \end{aligned} \quad (1)$$

where ξ is the nonconserved phase field order variable and ξ values of 1 and 0 are defined to represent the electrode phase and the electrolyte phase, respectively. We combined all of the terms related to interface energy and introduced a random perturbation to reflect the amorphous structure of the SEI and its effect on the direction of the interface kinetics,³⁰ where χ is a random number and ψ is the perturbation amplitude. Moreover, we also introduced the SEI restriction on the transport rate of ions and electrons in the interface (see the [Supporting Information](#)); hence, this model can fully reflect the known limitations of SEI on the interface kinetics (rate and direction). In addition, we introduce the lithium atom diffusion kinetics described by the conservative Cahn–Hilliard equation as a term into the equation to introduce the effect of atom diffusion on lithium electrodeposition. After the corrections described above and further incorporation of the ion transport equation, potential equation, and energy equation, this phase field model can comprehensively reflect the effects of ion transport, electrochemical reaction, atom diffusion, and SEI restriction on the lithium electrodeposition process. We transformed the optimized phase field model into its corresponding weak form so that we can solve such a system of multiorder nonlinear coupled partial differential equations. Other model and calculation details can be found in the [Supporting Information](#).

Figure 1 shows the effects of SEI and atom diffusion on the growth morphology of a single dendrite at 25 °C. At the beginning of deposition, a semi-elliptical initial nucleus is set on the anode side, as shown in **Figure 1a**. The y -axis is the major semi-axis, with a value of 0.1 μm , while the x -axis is the minor semi-axis, with a value of 0.0707 μm . The evolution of single dendrites over time without considering the effect of atom diffusion and SEI restriction on the direction of interface kinetics is shown in panels **c** and **d** of **Figure 1**. Due to the body-centered cubic crystal structure of lithium metal, the main branch of the dendrite splits into three parts and grows outward during the deposition process and further splits on the side of the main branch to form side branches. As the deposition proceeds, because the main branch upward can obtain the most sufficient lithium-ion supply, as depicted in **Figure S1**, the dendrite growth rate along this direction is the fastest. As the SEI restriction is not fully considered, the

deposition morphology is regular and symmetrical (**Figure 1c**), which is different from the random side branches observed in the experiment (**Figure 1b**).

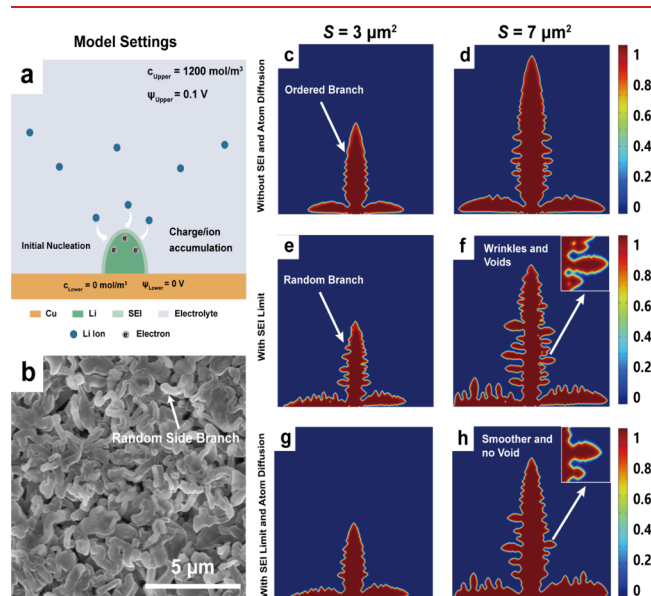


Figure 1. Single-dendrite morphology evolution under different conditions. (a) Model setup schematic. (b) SEM image of the lithium dendrite morphology. (c and d) Morphology without considering SEI restriction and atom diffusion. (e and f) Considering only SEI restriction. (g and h) Both effects considered.

The dendrite morphology evolution after considering the SEI restriction on the interface kinetics is shown in panels **e** and **f** of **Figure 1**. As depicted in **Figure 1e**, the main branch morphology is no longer symmetrical, and many random side branches appear on the dendrite, which can better reflect the random structure of the real lithium dendrite. The evolution of a single dendrite morphology when both factors are considered is shown in panels **g** and **h** of **Figure 1**. Although the atom diffusion effect is weak at room temperature, one can see that the surface microwrinkles and internal micropores are partially eliminated. Because the effect of atom diffusion will be significantly enhanced at high temperatures,^{29,39} it may have a

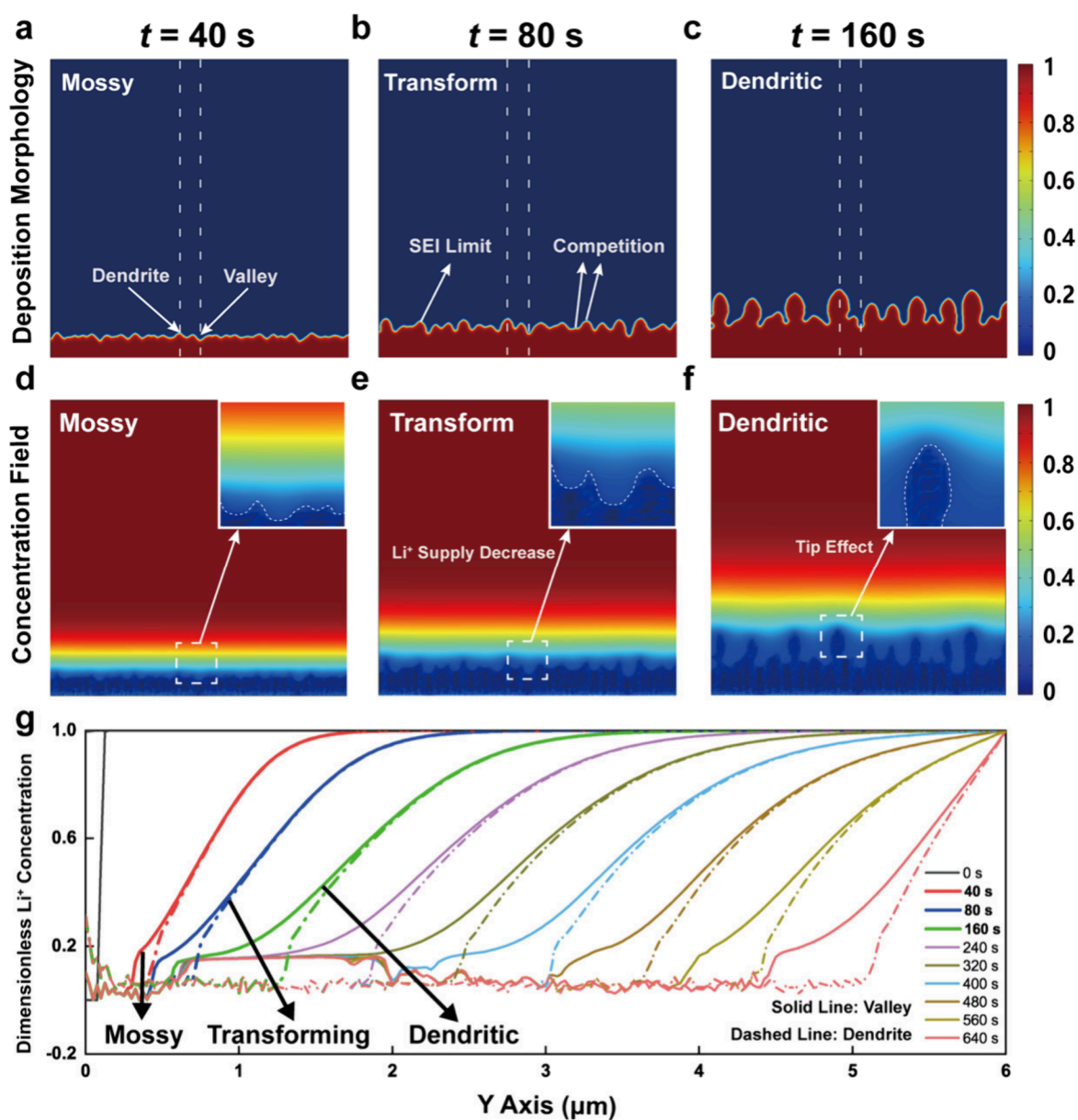


Figure 2. Transition of the lithium deposition morphology. (a–c) Evolution of morphology over time. (d–f) Corresponding concentration fields. (g) Line plots of Li⁺ concentration in the valley and dendrite regions.

significant impact on the deposition process, and therefore, it must be considered in the phase field model.

To deeply understand the lithium deposition mechanism at different temperature fields, we first studied the lithium deposition morphology transformation process and mechanism at 40 °C, as shown in Figure 2. The experimental study of Bai et al. showed that as lithium deposition proceeds, due to the decrease of Li⁺ supply and the unchanged applied voltage, the lithium deposition morphology will gradually change from a dense moss-like shape limited by the electrochemical reaction rate to a dendrite-like shape limited by the ion diffusion rate.¹⁵ As long as the deposition continues, the process described above is inevitable. The specific simulation verification results are shown in Figure 2. As depicted in Figure 2a–c, as the deposition proceeds, the lithium deposition morphology gradually changes from a flat moss-like shape to a distinct dendrite-like shape, and all sites almost change simultaneously, which is consistent with the previous experimental research

results.¹⁵ The corresponding concentration field distribution is given in Figure 2d–f. One can see that during the morphology transformation process, the Li⁺ supply will decrease around the dendrite and the tip effect will be more serious.

In addition, we took the intercepts of a valley and a dendrite region (Figure 2a) and plotted the corresponding concentration distribution curves over time in Figure 2g. In the early stage of lithium deposition (before 40 s), one can see from the concentration curve that the Li⁺ supply is sufficient and the corresponding deposition morphology is dense moss-like. As the deposition proceeds (after 40 s), the supply of Li⁺ continues to decrease. Due to the random perturbation of the interface kinetics caused by SEI, there is a competitive relationship between adjacent deposition sites. The Li⁺ supply at some sites gradually approaches a critical value after SEI restriction, and the corresponding deposition tends to stagnate; a platform appears in the concentration curve at the intercept. Those sites with advantages continue to be

deposited, and the corresponding intercept concentration curve is always in a fluctuating state. In the subsequent deposition process, the supply of Li^+ continues to decrease, and the tip effect becomes more obvious (see Figure 2f). More charges and Li^+ are gathered at the tip of some dominant dendrites, forming a dendritic deposition morphology. Moreover, we also simulated the case without considering the atom diffusion kinetics, as shown in Figure S3. We found that the time required for the deposition morphology transformation decreased and the critical concentration increased from 180 to 192 mol/m³, indicating that atom diffusion can help maintain the deposition morphology as a dense moss-like structure, delay the process of the deposition morphology transformation, and reduce the critical concentration for it, further proving the significance of considering this factor in the phase field model. Proper utilization of atom diffusion may provide important help for the stable operation of Li metal batteries.

Having verified the inevitability of the transformation of the lithium deposition process, we further studied the effect of ambient temperature on the lithium deposition process, as shown in Figure 3. In the low-temperature environment, the

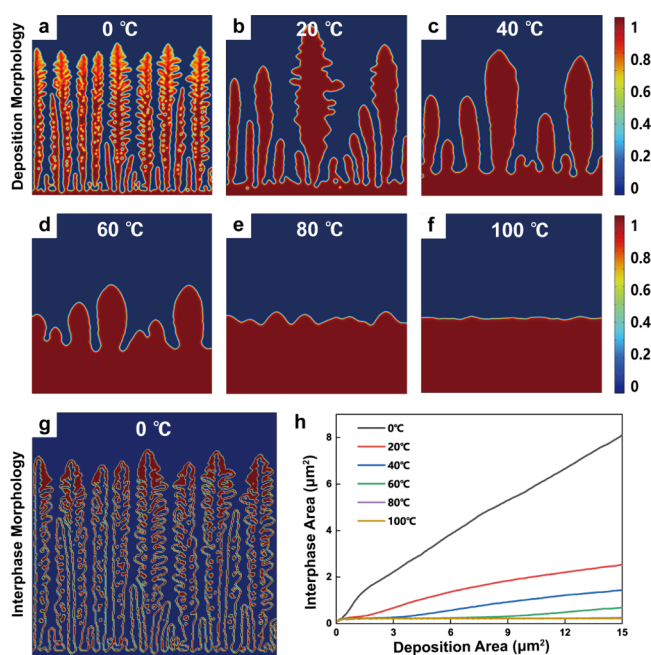


Figure 3. Lithium deposition morphology at different ambient temperatures and the same deposition amount (15 μm²). (a–f) Morphology under ambient temperatures of 0, 20, 40, 60, 80, and 100 °C, respectively. (g) Phase interface region at 0 °C. (h) Line plot of the interphase area as a function of deposition area at different ambient temperatures.

Li^+ supply reaches the critical value and the deposition morphology changes to a dendrite shape at a very small deposition amount (Figure 3a). As the temperature increases, the diffusion rate inside the battery accelerates exponentially (Arrhenius correlation), and the moss-like deposition morphology can still be maintained under a large deposition amount (Figure 3f). An adequate Li^+ supply ensures that the deposition remains in a moss-like shape limited by the electrochemical reaction rate, and rapid atom diffusion tends to keep the deposition specific surface area at a minimum, further ensuring the flatness of lithium deposition. The results without considering atom diffusion are shown in Figure S4. At

low temperatures, the atom diffusion kinetics is weak and the deposition morphologies are slightly different. As the ambient temperature increases, the number of voids decreases greatly but the deposition amount required for the morphology transformation also continues to increase, indicating that atom diffusion kinetics plays a vital role in the lithium electro-deposition process.

Moreover, the order variable in the range of 0.2–0.8 is taken as the phase interface to quantitatively study the effect of ambient temperature on lithium deposition, as shown in Figure 3g. The corresponding phase interface area over the amount of deposition is shown in Figure 3h. The interphase area can reflect the amount of Li^+ consumed by the side reaction to generate the solid electrolyte interface. One can clearly see that the specific surface area of lithium deposition decreases significantly as the temperature increases, which is beneficial to the long-term stable cycling of lithium metal batteries.²⁸ It should be noted that as we introduced the random perturbation of interface kinetics by SEI, the deposition morphology presents a very random structure, which is more consistent with the real dendrite morphologies observed in experiment.²⁹ In addition, on the basis of the previous definition of the phase interface, we measured the thickness of the interface layer at several locations, which was approximately 35–40 nm and very close to the SEI thickness observed in the experiment using cryo-electron microscopy.³⁰

We further explored the influence of a local hot spot inside the battery on lithium deposition, as shown in Figure 4. Through experimental studies, Zhu et al. found that local hot spots inside the battery will cause the acceleration of local deposition, which may lead to short circuit problems inside the battery.⁸ Here we used the optimized phase field model to deeply analyze the influence and mechanism of local hot spots on the lithium deposition morphology. Some parameters were modified so that we can show the impact of a local hot spot in a calculation domain smaller than a real battery (see the Supporting Information for more details). Under a square hot spot (100 nm × 100 nm), the temperature field near the hot spot is more concentrated (Figure 4a). As the deposition proceeds, an obvious tip effect occurs, and many charges and ions accumulate above the hot spot, leading to accelerated deposition at this site (Figure S5). The morphology shows an obvious dendritic shape (Figure 4c). Under a rectangle local hot spot (500 nm × 50 nm), the temperature field near the hot spot is more uniform (Figure 4b), the tip effect above the hot spots is significantly alleviated, and the uniformity of the deposition morphology is significantly improved (Figure 4d). One can see from the corresponding phase interface area changing curve that with the “dilution” of local hot spots, the specific surface area of lithium deposition is significantly reduced (Figure 4e), which is conducive to the long-term stable operation of lithium metal batteries and consistent with previous experimental results.⁴⁷

In conclusion, we optimized the previous phase field model to comprehensively study the lithium deposition mechanism under different conditions. The results show that after considering the SEI restrictions and atom diffusion, the deposition can be closer to the actual morphology. Through calculation, we verified the inevitability of lithium deposition morphology transforming from mossy to dendritic and proved the significance of model optimization on it. We found that with an increase in ambient temperature the deposition amount required for the transformation can be increased,

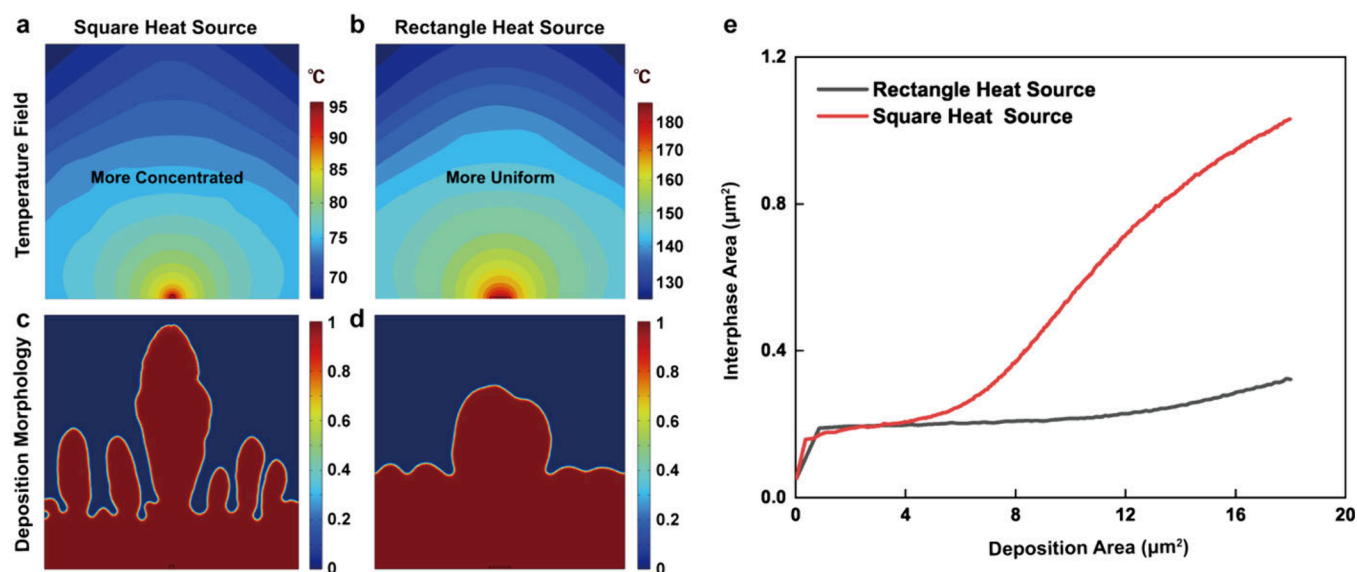


Figure 4. Temperature field and corresponding deposition results with different hot spot shapes. (a and b) Temperature field under square (100 nm \times 100 nm) and rectangle (500 nm \times 50 nm) hot spots, respectively. (c and d) Corresponding deposition morphologies. (e) Line plot of the interphase area as a function of deposition area under different hot spots.

which is beneficial to battery cycling. Moreover, our results show that with the “dilution” of the local hot spot, the tip effect above the hot spot can be alleviated, inhibiting the formation of lithium dendrites, which is conducive to the stable operation of the battery. It is worth noting that the mechanical properties and fracture problems of SEI have not been considered in our model, which is also one of the issues worth studying. In addition, the battery temperature cannot be increased infinitely under actual conditions to keep it from failing. Our model can conveniently and relatively accurately simulate the lithium deposition morphology under various conditions. We hope it could provide aid for further exploring thermally regulated stable operation of lithium metal batteries.

■ ASSOCIATED CONTENT

SI Supporting Information

The Supporting Information is available free of charge at <https://pubs.acs.org/doi/10.1021/acs.nanolett.4c06505>.

Detailed model and simulation setup information, parameters used in the simulation, supporting concentration field, and lithium deposition simulations without considering atom diffusion kinetics (PDF)

■ AUTHOR INFORMATION

Corresponding Author

Yucan Peng – Department of Energy and Resources Engineering, College of Engineering, Peking University, Beijing 100871, P. R. China; orcid.org/0009-0008-4908-0319; Email: yucan.peng@pku.edu.cn

Authors

Guowei Tang – Department of Energy and Resources Engineering, College of Engineering, Peking University, Beijing 100871, P. R. China; orcid.org/0009-0006-1583-9273

Libo Men – State Key Lab for Strength and Vibration of Mechanical Structures, Department of Engineering Mechanics, Xi'an Jiaotong University, Xi'an 710049, P. R. China

Yilin Wang – Department of Energy and Resources Engineering, College of Engineering, Peking University, Beijing 100871, P. R. China

Rong Xu – State Key Lab for Strength and Vibration of Mechanical Structures, Department of Engineering Mechanics, Xi'an Jiaotong University, Xi'an 710049, P. R. China

Complete contact information is available at: <https://pubs.acs.org/doi/10.1021/acs.nanolett.4c06505>

Author Contributions

Y.P. and G.T. conceived the idea. G.T. derived the optimized equation and built up the simulation model with the help of L.M., Y.W., and R.X. Y.P. supervised the project. All authors discussed results and commented on the manuscript.

Notes

The authors declare no competing financial interest.

■ ACKNOWLEDGMENTS

This work was supported by the National Natural Science Foundation of China (Grants 22475007 and 12302232). The authors thank Jing Wang for providing the experimental image of Li dendrites.

■ REFERENCES

- (1) Lin, D.; Liu, Y.; Cui, Y. Reviving the Lithium Metal Anode for High-Energy Batteries. *Nat. Nanotechnol.* **2017**, *12*, 194–206.
- (2) Zhang, Y.; Zuo, T. T.; Popovic, J.; Lim, K.; Yin, Y. X.; Maier, J.; Guo, Y. G. Towards Better Li Metal Anodes: Challenges and Strategies. *Mater. Today* **2020**, *33*, 56–74.
- (3) Cheng, X. B.; Zhang, R.; Zhao, C. Z.; Zhang, Q. Toward Safe Lithium Metal Anode in Rechargeable Batteries: A Review. *Chem. Rev.* **2017**, *117*, 10403–10473.
- (4) Liang, Y.; Dong, H.; Aurbach, D.; Yao, Y. Current Status and Future Directions of Multivalent Metal-Ion Batteries. *Nature Energy* **2020**, *5*, 646–656.
- (5) Choi, J. W.; Aurbach, D. Promise and Reality of Post-Lithium-Ion Batteries with High Energy Densities. *Nat. Rev. Mater.* **2016**, *1*, 16013.

- (6) Kwak, W. J.; Rosy, N.; Sharon, D.; Xia, C.; Kim, H.; Johnson, L. R.; Bruce, P. G.; Nazar, L. F.; Sun, Y. K.; Frimer, A. A.; Noked, M.; Freunberger, S. A.; Aurbach, D. Lithium-Oxygen Batteries and Related Systems: Potential, Status, and Future. *Chem. Rev.* **2020**, *120*, 6626–6683.
- (7) Krauskopf, T.; Richter, F. H.; Zeier, W. G.; Janek, J. Physicochemical Concepts of the Lithium Metal Anode in Solid-State Batteries. *Chem. Rev.* **2020**, *120*, 7745–7794.
- (8) Zhu, Y.; Xie, J.; Pei, A.; Liu, B.; Wu, Y.; Lin, D.; Li, J.; Wang, H.; Chen, H.; Xu, J.; Yang, A.; Wu, C. L.; Wang, H.; Chen, W.; Cui, Y. Fast Lithium Growth and Short Circuit Induced by Localized-Temperature Hotspots in Lithium Batteries. *Nat. Commun.* **2019**, *10*, 2067.
- (9) Xiang, Y.; Tao, M.; Chen, X.; Shan, P.; Zhao, D.; Wu, J.; Lin, M.; Liu, X.; He, H.; Zhao, W.; Hu, Y.; Chen, J.; Wang, Y.; Yang, Y. Gas Induced Formation of Inactive Li in Rechargeable Lithium Metal Batteries. *Nat. Commun.* **2023**, *14*, 117.
- (10) Rojaee, R.; Shahbazian-Yassar, R. Two-Dimensional Materials to Address the Lithium Battery Challenges. *ACS Nano* **2020**, *14*, 2628–2658.
- (11) Wang, Q.; Zhao, C.; Wang, S.; Wang, J.; Liu, M.; Ganapathy, S.; Bai, X.; Li, B.; Wagemaker, M. Clarifying the Relationship between the Lithium Deposition Coverage and Microstructure in Lithium Metal Batteries. *J. Am. Chem. Soc.* **2022**, *144*, 21961–21971.
- (12) Raj, V.; Venturi, V.; Kankanallu, V. R.; Kuri, B.; Viswanathan, V.; Aetukuri, N. P. B. Direct Correlation between Void Formation and Lithium Dendrite Growth in Solid-State Electrolytes with Interlayers. *Nat. Mater.* **2022**, *21*, 1050–1056.
- (13) Bai, P.; Guo, J.; Wang, M.; Kushima, A.; Su, L.; Li, J.; Brushett, F. R.; Bazant, M. Z. Interactions between Lithium Growths and Nanoporous Ceramic Separators. *Joule* **2018**, *2*, 2434–2449.
- (14) He, Y.; Ren, X.; Xu, Y.; Engelhard, M. H.; Li, X.; Xiao, J.; Liu, J.; Zhang, J. G.; Xu, W.; Wang, C. Origin of Lithium Whisker Formation and Growth under Stress. *Nat. Nanotechnol.* **2019**, *14*, 1042–1047.
- (15) Bai, P.; Li, J.; Brushett, F. R.; Bazant, M. Z. Transition of Lithium Growth Mechanisms in Liquid Electrolytes. *Energy Environ. Sci.* **2016**, *9*, 3221–3229.
- (16) Zhang, X.; Yang, Y.; Zhou, Z. Towards Practical Lithium-Metal Anodes. *Chem. Soc. Rev.* **2020**, *49*, 3040–3071.
- (17) Qian, J.; Henderson, W. A.; Xu, W.; Bhattacharya, P.; Engelhard, M.; Borodin, O.; Zhang, J. G. High Rate and Stable Cycling of Lithium Metal Anode. *Nat. Commun.* **2015**, *6*, 6362.
- (18) Zheng, J.; Engelhard, M. H.; Mei, D.; Jiao, S.; Polzin, B. J.; Zhang, J. G.; Xu, W. Electrolyte Additive Enabled Fast Charging and Stable Cycling Lithium Metal Batteries. *Nat. Energy* **2017**, *2*, 17012.
- (19) Zhang, Y.; Hua, Y.; Zhao, G.; Tu, F.; Li, T.; Li, M. G.; Fu, L.; Yang, C.; Tang, A.; Yang, H. Separators Modified with Ultrathin Montmorillonite/Polymer Nanocoatings Achieve Dendrite-Free Lithium Deposition at High Current Densities. *Nano Lett.* **2024**, *24*, 8834–8842.
- (20) Qu, Z.; Chen, K.; Wang, W.; Dai, Y.; Lu, X.; Lyu, S. S. Interfacial Layers with Desolvation Function Induced Stable Deposition of Lithium Metal for Long-Cycling Lithium Metal Batteries. *Nano Lett.* **2024**, *24*, 8055–8062.
- (21) Wan, H.; Xu, J.; Wang, C. Designing Electrolytes and Interphases for High-Energy Lithium Batteries. *Nature Reviews Chemistry* **2024**, *8*, 30–44.
- (22) Wang, Y.; Wu, Z.; Azad, F. M.; Zhu, Y.; Wang, L.; Hawker, C. J.; Whittaker, A. K.; Forsyth, M.; Zhang, C. Fluorination in Advanced Battery Design. *Nature Reviews Materials* **2024**, *9*, 119–133.
- (23) Wang, H.; Wei, P.; Wang, J.; Wang, D. Hollow Multishelled Structure Reviving Lithium Metal Anode for High-Energy-Density Batteries. *Chemical Research in Chinese Universities* **2024**, *40*, 428–436.
- (24) Wei, P.; Wang, H.; Yang, M.; Wang, J.; Wang, D. Relocatable Hollow Multishelled Structure-Based Membrane Enables Dendrite-Free Lithium Deposition for Ultraprecise Lithium Metal Batteries. *Adv. Energy Mater.* **2024**, *14*, 2400108.
- (25) Chang, C.; Zhang, M.; Lao, Z.; Xiao, X.; Lu, G.; Qu, H.; Wu, X.; Fu, H.; Zhou, G. Achieving Stable Lithium Anodes through Leveraging Inevitable Stress Variations via Adaptive Piezoelectric Effect. *Adv. Mater.* **2024**, *36*, 2313525.
- (26) Lu, G.; Wu, X.; Huang, M.; Zhang, M.; Piao, Z.; Zhong, X.; Li, C.; Song, Y.; Chang, C.; Yu, K.; Zhou, G. A Self-Adsorption Molecule Passivated Interface Enables Efficient and Stable Lithium Metal Batteries. *Energy Environ. Sci.* **2024**, *17*, 9555–9565.
- (27) Zhang, M. T.; Qu, H. T.; Zhou, G. M. The Factors That Influence the Electrochemical Behaviors of Lithium Metal Anodes: Electron Transfer and Li-Ion Transport. *New Carbon Materials* **2023**, *38*, 776–786.
- (28) Yan, K.; Wang, J.; Zhao, S.; Zhou, D.; Sun, B.; Cui, Y.; Wang, G. Temperature-Dependent Nucleation and Growth of Dendrite-Free Lithium Metal Anodes. *Angewandte Chemie - International Edition* **2019**, *58*, 11364–11368.
- (29) Li, L.; Basu, S.; Wang, Y.; Chen, Z.; Hundekar, P.; Wang, B.; Shi, J.; Shi, Y.; Narayanan, S.; Koratkar, N. Self-Heating-Induced Healing of Lithium Dendrites. *Science* **2018**, *359*, 1513–1516.
- (30) Wang, J.; Huang, W.; Pei, A.; Li, Y.; Shi, F.; Yu, X.; Cui, Y. Improving Cyclability of Li Metal Batteries at Elevated Temperatures and Its Origin Revealed by Cryo-Electron Microscopy. *Nat. Energy* **2019**, *4*, 664–670.
- (31) Wang, H.; Zhu, Y.; Kim, S. C.; Pei, A.; Li, Y.; Boyle, D. T.; Wang, H.; Zhang, Z.; Ye, Y.; Huang, W.; Liu, Y.; Xu, J.; Li, J.; Liu, F.; Cui, Y. Underpotential Lithium Plating on Graphite Anodes Caused by Temperature Heterogeneity. *Proc. Natl. Acad. Sci. U. S. A.* **2020**, *117*, 29453–29461.
- (32) Tao, M.; Chen, X.; Lin, H.; Jin, Y.; Shan, P.; Zhao, D.; Gao, M.; Liang, Z.; Yang, Y. Clarifying the Temperature-Dependent Lithium Deposition/Stripping Process and the Evolution of Inactive Li in Lithium Metal Batteries. *ACS Nano* **2023**, *17*, 24104–24114.
- (33) Thenuwara, A. C.; Shetty, P. P.; McDowell, M. T. Distinct Nanoscale Interphases and Morphology of Lithium Metal Electrodes Operating at Low Temperatures. *Nano Lett.* **2019**, *19*, 8664–8672.
- (34) Sano, H.; Kitta, M.; Shikano, M.; Matsumoto, H. Effect of Temperature on Li Electrodeposition Behavior in Room-Temperature Ionic Liquids Comprising Quaternary Ammonium Cation. *J. Electrochem. Soc.* **2019**, *166*, A2973–A2979.
- (35) Akolkar, R. Modeling Dendrite Growth during Lithium Electrodeposition at Sub-Ambient Temperature. *J. Power Sources* **2014**, *246*, 84–89.
- (36) Thenuwara, A. C.; Shetty, P. P.; Kondekar, N.; Sandoval, S. E.; Cavallaro, K.; May, R.; Yang, C. T.; Marbella, L. E.; Qi, Y.; McDowell, M. T. Efficient Low-Temperature Cycling of Lithium Metal Anodes by Tailoring the Solid-Electrolyte Interphase. *ACS Energy Lett.* **2020**, *5*, 2411–2420.
- (37) Vishnugopi, B. S.; Hao, F.; Verma, A.; Mukherjee, P. P. Double-Edged Effect of Temperature on Lithium Dendrites. *ACS Appl. Mater. Interfaces* **2020**, *12*, 23931–23938.
- (38) Hong, Z.; Viswanathan, V. Prospect of Thermal Shock Induced Healing of Lithium Dendrite. *ACS Energy Lett.* **2019**, *4*, 1012–1019.
- (39) Jiao, J.; Lai, G.; Zhao, L.; Lu, J.; Li, Q.; Xu, X.; Jiang, Y.; He, Y. B.; Ouyang, C.; Pan, F.; Li, H.; Zheng, J. Self-Healing Mechanism of Lithium in Lithium Metal. *Adv. Sci.* **2022**, *9*, 2105574.
- (40) Hong, Z.; Viswanathan, V. Phase-Field Simulations of Lithium Dendrite Growth with Open-Source Software. *ACS Energy Lett.* **2018**, *3*, 1737–1743.
- (41) Zhang, Y.; Li, Y.; Shen, W.; Li, K.; Lin, Y. Important Role of Atom Diffusion in Dendrite Growth and the Thermal Self-Healing Mechanism. *ACS Appl. Energy Mater.* **2023**, *6*, 1933–1945.
- (42) Jeon, J.; Yoon, G. H.; Vegge, T.; Chang, J. H. Phase-Field Investigation of Lithium Electrodeposition at Different Applied Overpotentials and Operating Temperatures. *ACS Appl. Mater. Interfaces* **2022**, *14*, 15275–15286.
- (43) Li, Y.; Zhao, W.; Zhang, G.; Shi, S. Unified Picture on Temperature Dependence of Lithium Dendrite Growth via Phase-Field Simulation. *Energy Mater.* **2023**, *4*, 0053.

(44) Chen, L.; Zhang, H. W.; Liang, L. Y.; Liu, Z.; Qi, Y.; Lu, P.; Chen, J.; Chen, L. Q. Modulation of Dendritic Patterns during Electrodeposition: A Nonlinear Phase-Field Model. *J. Power Sources* **2015**, *300*, 376–385.

(45) Yan, H. H.; Bie, Y. H.; Cui, X. Y.; Xiong, G. P.; Chen, L. A Computational Investigation of Thermal Effect on Lithium Dendrite Growth. *Energy Convers Manag* **2018**, *161*, 193–204.

(46) Moelans, N.; Blanpain, B.; Wollants, P. An Introduction to Phase-Field Modeling of Microstructure Evolution. *Calphad* **2008**, *32*, 268–294.

(47) Han, D.; Wang, X.; Zhou, Y. N.; Zhang, J.; Liu, Z.; Xiao, Z.; Zhou, J.; Wang, Z.; Zheng, J.; Jia, Z.; Tian, B.; Xie, J.; Liu, Z.; Tang, W. A Graphene-Coated Thermal Conductive Separator to Eliminate the Dendrite-Induced Local Hotspots for Stable Lithium Cycling. *Adv. Energy Mater.* **2022**, *12*, 2201190.